In situ Raman studies of single-walled carbon nanotubes grown by local catalyst heating

Cite as:
Dittmer, S., Olofsson, N., Weis, J. E., Nerushev, O., Gromov, A., & Campbell, E. (2008). In situ Raman studies of single-walled carbon nanotubes grown by local catalyst heating. *Chemical Physics Letters*, 457(1-3), 206-210.

Manuscript received: 15/01/2008; Accepted: 02/04/2008; Article published: 06/04/2008

In situ Raman studies of single-walled carbon nanotubes grown by local catalyst heating**

S. Dittmer,[1] N. Olofsson,[1] J. Ek Weis,[1,2] O.A. Nerushev,[2] A.V. Gromov[2] and E.E.B. Campbell[1,2,*]

[1]Dept. of Physics, Göteborg University, SE-41296 Göteborg, Sweden.

[2]EaStCHEM, School of Chemistry, Joseph Black Building, University of Edinburgh, West Mains Road, Edinburgh, EH9 3JJ, UK.

[*]Corresponding author; e-mail: Eleanor.Campbell@ed.ac.uk

[**]The authors thank Lena Falk and Shantenu Mudgal for help with the TEM studies. Financial support from the Swedish Research Council, the Swedish Strategic Research Foundation (SSF) and from the EU via the NANORF STREP project is gratefully acknowledged. This paper reflects the views of the authors and not necessarily those of the EC. The community is not liable for any use that may be made of the information contained herein.

Abstract

Using *in-situ* Raman spectroscopy we investigate single wall carbon nanotube growth on Mo electrodes, using a highly localized resistive heating technique. Small diameter semiconducting single wall nanotubes grow very rapidly when the catalyst support is heated to a temperature of 800 ^{o}C. The G/D ratio shows an interesting time-dependent behaviour. It first decreases, indicating the presence of amorphous carbon and then significantly increases again after ca. 5 minutes growth while retaining the position and shape expected for predominantly semiconducting carbon nanotubes.

1. Introduction

Carbon nanotubes have been intensively studied for over fifteen years, however, the field still lacks a comprehensive understanding of the detailed processes behind carbon nanotube growth. Many questions concerning the growth mechanisms, the reasons for the cessation of growth and possibility of chiral control remain to be answered. *In situ* investigations can shed light on the kinetics and mechanisms of nanotube growth and provide important information for detailed modelling studies and development of highly controlled growth. Such studies have been performed in recent years for laser vaporisation growth [1,2], cold wall chemical vapour deposition (CVD) [3,4], XPS studies [5], microbalance studies [6] and plasma-enhanced CVD growth of nanotubes and nanofibres [7,8] to achieve a more detailed understanding by observing the tubes or their environment directly during growth. Here, using an in-house developed resistive growth method that locally heats the catalyst, keeping the rest of the substrate at low temperatures (< 100 ^{o}C) , [9], we study the growth of single walled carbon nanotubes using *in situ* Raman spectroscopy.

In-situ Raman spectroscopy of nanotubes grown by chemical vapor deposition has so far mainly been focused on investigating the D-G band of carbon nanotubes – in most cases with the aim of determining the amount of carbon nanotubes present from following the evolution of the integrated G-band area [3,4]. Chiasi et al. [3] showed that the integrated G-band intensity increased linearly with time after growth initiation which could be due to a linear increase of the nanotube length or an increase in nanotube nucleation with time. Kaminska et al. [4] used Raman imaging to observe the appearance of carbon nanotubes with time and estimate the growth rate to be 7 μm/s or higher.

Our main interest has been the short time dynamics, looking at the onset of growth and investigating the diameter distribution of the nanotubes as a function of time. To this end we have developed a method which allows unprecedented control of growth time compared with all other CVD methods and, at the same time, makes it possible to access the immediate growth zone using a micro-Raman spectrometer.

The technique of using resistive heating to locally grow carbon nanotubes has been exploited by other groups for growing multi-walled nanotubes (MWNT) on silicon cantilevers, particularly for NEMS applications

[10,11]. We follow a simplified and more flexible approach where a metal electrode deposited directly on a silicon chip is used as a nano- or micro-scale heater. This allows us to grow nanotubes directly on contact electrodes. An additional advantage is that we can also easily switch between multi-walled and single-walled nanotubes by adjusting the growth conditions [9,12].

2. Experimental Setup

In the present study we use local resistive heating to grow high quality single walled nanotubes. Molybdenum electrodes are patterned on standard silicon wafers with a 2μm thick layer of oxide. In earlier work we used tungsten as electrode material [9]. The electrode is designed to be strongly heated in a small region when passing a sufficiently high current through the material. Some examples of electrodes can be seen in Figure 1. The samples are prepared using standard e-beam lithography and thin film deposition in a lift off process. The electrode material is deposited using electron beam evaporation and typically consists of 100 nm thick Mo with 5 nm Ti as adhesion layer between the Mo and silicon dioxide. In a second lithography step, a thin film catalyst is deposited in rectangular areas on the heater. The catalyst used in the present studies is 1 nm iron, Fe, supported on 5 nm Al_2O_3.

To be able to perform nanotube growth under a microscope, a dedicated growth chamber was designed to fit on the stage of a Renishaw InVia Raman spectrometer. The chamber has a total volume of 200 cm^3 and the growth zone on the sample is accessible optically through a quartz window using a long working distance x50 objective. Electrical connections to the molybdenum pads on the substrate are made using gold coated needles inside the chamber.

In a typical growth process the chamber is first pumped to high vacuum conditions using a small turbomolecular pump and then flushed with argon a few times before maintaining a flow of 300 sccm H_2, and 500 sccm Ar at atmospheric pressure. The catalytically active site on the substrate is heated by stepwise ramping up the current through the Mo heater to reach the optimum growth current (dependent on the actual electrode geometry) on a timescale of approximately 4 minutes. Immediately before growth the chamber is sealed and evacuated before 6 sccm of ethylene is then added to the gas mixture in the feeding line. Due to the chamber being sealed off, a slight overpressure builds up in the feeder line which allows immediate filling of the growth chamber volume as soon as the feeder valve is reopened.

During the first few seconds of ethylene exposure, a rapid change in resistivity is experienced in the active region. This is manifested as a sudden increase in the voltage drop along the heater. This resistivity change is most probably due to a carbidisation of the electrode material resulting in a higher resistivity accompanied by an increase in resistive heating.

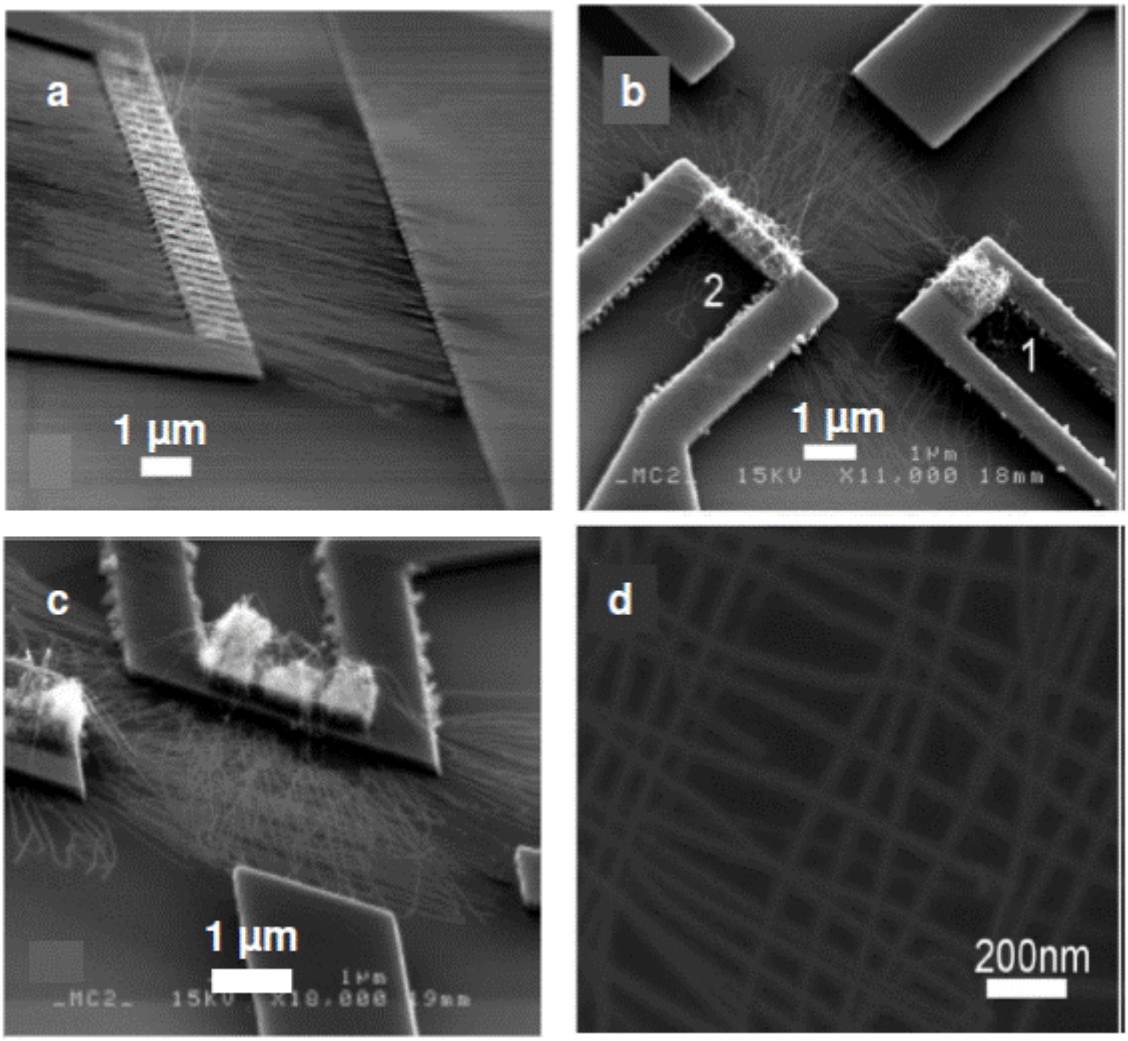

Figure 1. Examples of SWNT arrays grown from Mo electrodes using the local heating method (ethylene hydrocarbon precursor with Fe catalyst). The substrates were tilted by 20°. (a) SWNT aligned during growth in the presence of a DC electric field (1 V/lm) (b) and (c) sequential growth of SWNT arrays. In (c) small vertically aligned MWNT arrays were first grown as the electrode temperature was increased. (d) Magnification of crossed SWNT from (b).

The temperature of the Mo heater can be determined by using the micro-Raman spectrometer to detect the emitted black-body radiation. The spectrometer was calibrated using a tungsten lamp. Examples are shown in Figure 2 for a heater with dimensions 30µm x 2 µm. Such measurements allow us to calibrate the current-temperature behaviour for different electrode geometries and precursor gases. Figure 2(a) and 2(b) show the results of measurements when the electrode was heated in the presence of Ar/H_2 but without any ethylene. The spectra can be fitted very well with the blackbody formula, $I(\lambda,T) = 2hc^2 / \lambda^5 \left(e^{hc/\lambda kT} - 1\right)^{-1}$, where h is Planck's constant, c the speed of light, λ the wavelength, k Boltzmann's constant and T the temperature. The fits yield temperatures of 700 ± 20 °C and 790 ±10 °C for 22 mA and 24 mA current, respectively. Figure 2(c)

shows what happens to the temperature of the heater as soon as the hydrocarbon precursor gas (ethylene) is added. There is a very significant increase in temperature from 790 ^{o}C to 910 ^{o}C. This temperature rise can also be clearly observed through the microscope objective as an increase in the intensity of the emitted light. The increase in temperature occurs simultaneously with the change in the voltage drop across the heater, discussed above, indicating a change in resistivity. This change is permanent since we observe that the temperature remains constant when the ethylene gas is turned off again. As we have shown previously [9,12], the temperature gradient close to the heater is very high, on the order of 100 ^{o}C /μm which means that the nanotube growth is restricted to the highly localised hot zone on the heater.

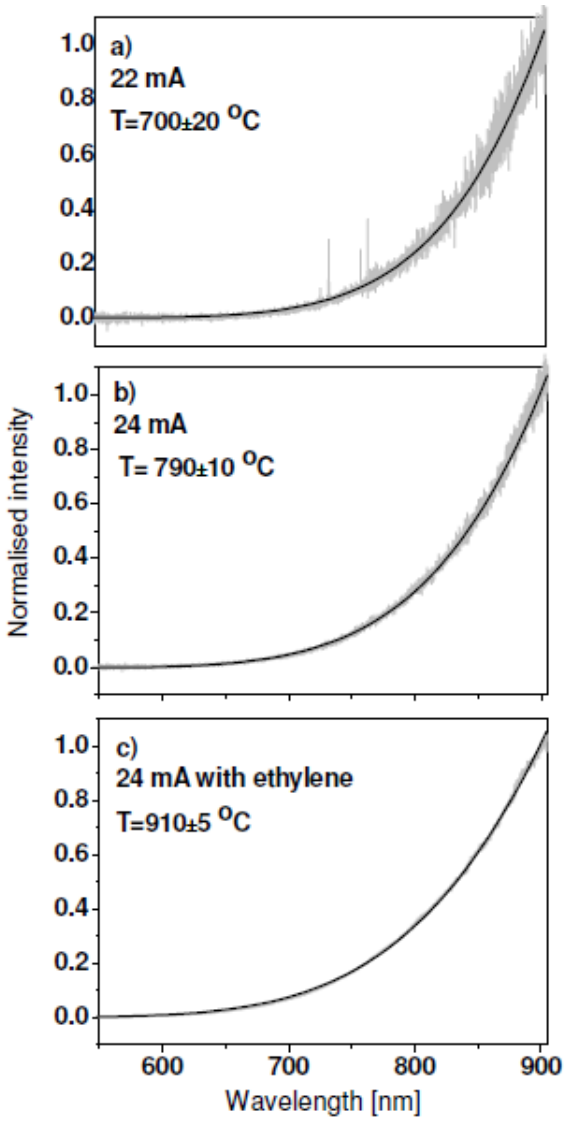

Figure 2. Blackbody radiation measurements to determine the temperature of the local heater. (a, b) Measurements made before the introduction of the hydrocarbon precursor for electrode currents of 22 mA and 24 mA, respectively. (c)Measurement made after introduction of ethylene for a current of 24 mA. The blackbody formula (see text) was fitted to the data yielding the temperatures given on the plots.

Growth is performed for the desired time, at the end of which the chamber is evacuated and the current is abruptly turned down to 10 mA, thus reducing the electrode temperature to well below the growth temperature window but still allowing growth to be efficiently restarted when the temperature is increased again. The reason for this procedure is to ensure a reasonably good Raman signal from the nanotubes that allows us to detect the radial breathing mode of individual SWNT and obtain a high signal/noise ratio for the D and G peaks. At high temperatures, such as those needed for growth, the intensities of the radial breathing modes and G-peaks of carbon nanotubes decrease dramatically.

The Raman measurements were carried out for four different excitation wavelengths (514 nm, 568 nm, 647 nm and 785 nm). The laser spot size was approximately 3 μm, focused on the growth electrode, and the power was kept below 1 $mW/\mu m^2$.

3. Results and Discussion

The examples of ethylene grown nanotubes shown in Figure 1 give an indication of the potential of the local heating growth method for device fabrication. In Figure 1(a) an array of horizontally aligned SWNT has been grown with the help of an aligning electrode providing an electric field during growth of 1V/μm. Since one can easily determine where nanotubes will grow by directing the heating current accordingly, one also has the possibility of carrying out sequential growth steps. This is illustrated in Figs. 1(b), (c) and (d). Growth was performed at a local catalyst temperature of ca. 900 ^{o}C. Two pairs of heater and aligning electrodes were patterned on the chip. In Figure 1(b) nanotubes were first grown from heater 1 towards the alignment electrode in the top left hand corner. After 5 minutes of growth, the heating current was switched off and heater 2 was switched on. The second array of nanotubes was grown from the bottom left to the top right hand corner. Empirically, we determined that an AC electric field was more effective for alignment. An extract from the central region of the crossed nanotubes is shown in Figure 1(d). It can be seen that the second set of grown tubes lies on top of the first set, creating a relatively dense mesh of tubes. If the heating current is turned on after the precursor gas is introduced (instead of introducing the precursor gas after the desired temperature has been reached) then it is possible to grow vertically aligned arrays of MWNT at lower temperatures. The MWNT growth is extremely efficient and occurs over a time period of only a few seconds. This is illustrated in Figure 1(c) where pillars of MWNT can be seen on the heater electrodes with SWNT growing over the tops of the pillars once a sufficiently high temperature has been reached. A similar effect was exploited by Bond [13] to grow suspended SWNT on top of MWNT pillars in a standard thermal CVD experiment by adjusting the global growth temperature. They further used this technique to grow a nanotube field effect transistor with a suspended tube as channel contacted at the source and drain by MWNT pillars [14]. The growth of vertical arrays of MWNT using our local heating technique will be the subject of a forthcoming article.

In order to obtain TEM images of our grown nanotubes, substrates were designed containing a small slit over which the nanotubes could be grown (Figure 3(b)). An example of a TEM image (obtained at 200 kV using a Philips CM200 microscope) of a small bundle of 2 SWNT is shown in Figure 3(a). Here the diameter of the nanotubes is 1.5 nm. It appears to be a common feature that SWNT growing across a gap will join together. A smaller resolution SEM picture in Figure 3(c) shows this effect very clearly.

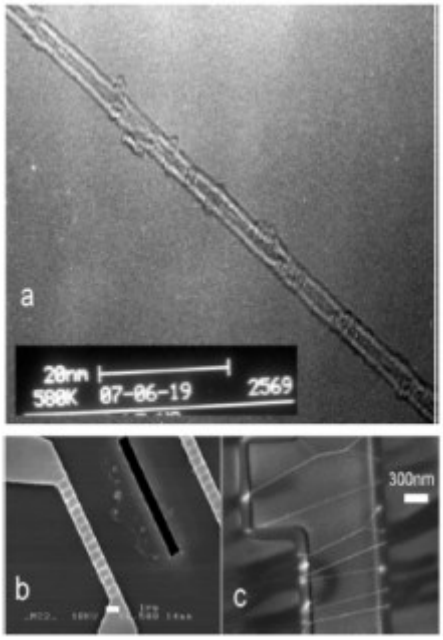

Figure 3. (a) TEM picture of SWNT crossing a slit in the growth substrate (200 kV, Philips CM200), (b) SEM picture of the substrate used for these studies, (c) SEM picture of SWNT grown across a slit, showing the tendency of the nanotubes to bundle as they cross.

In situ Raman experiments were carried out for growth at a local catalyst temperature of ca. 800 ^{o}C using the procedure described in section 2. In this case no aligning electric field was applied during growth. The results are summarised in Figure 4. Figure 4(a) shows the low wavenumber range of the spectra containing the RBM obtained for four different laser excitation wavelengths. The spectra were obtained after 5s, 15s, 1 minute, 5 minutes and 10 minutes growth time. Corresponding SEM images of the substrates are shown in Figure 4(c). It is clear from both the Raman spectra in Figure 4(a) and the SEM images that small diameter SWNT grow very quickly and can be seen growing out from the electrode even after 5s with a growth rate of at least 1 μm per second. As the growth time increases, the RBM region of the Raman spectra become more dense and the distribution of nanotube diameters represented by the RBM peaks broadens and, in particular, appears to shift to lower wavenumbers, i.e. larger diameter. An indication of this can also be seen in the SEM images.

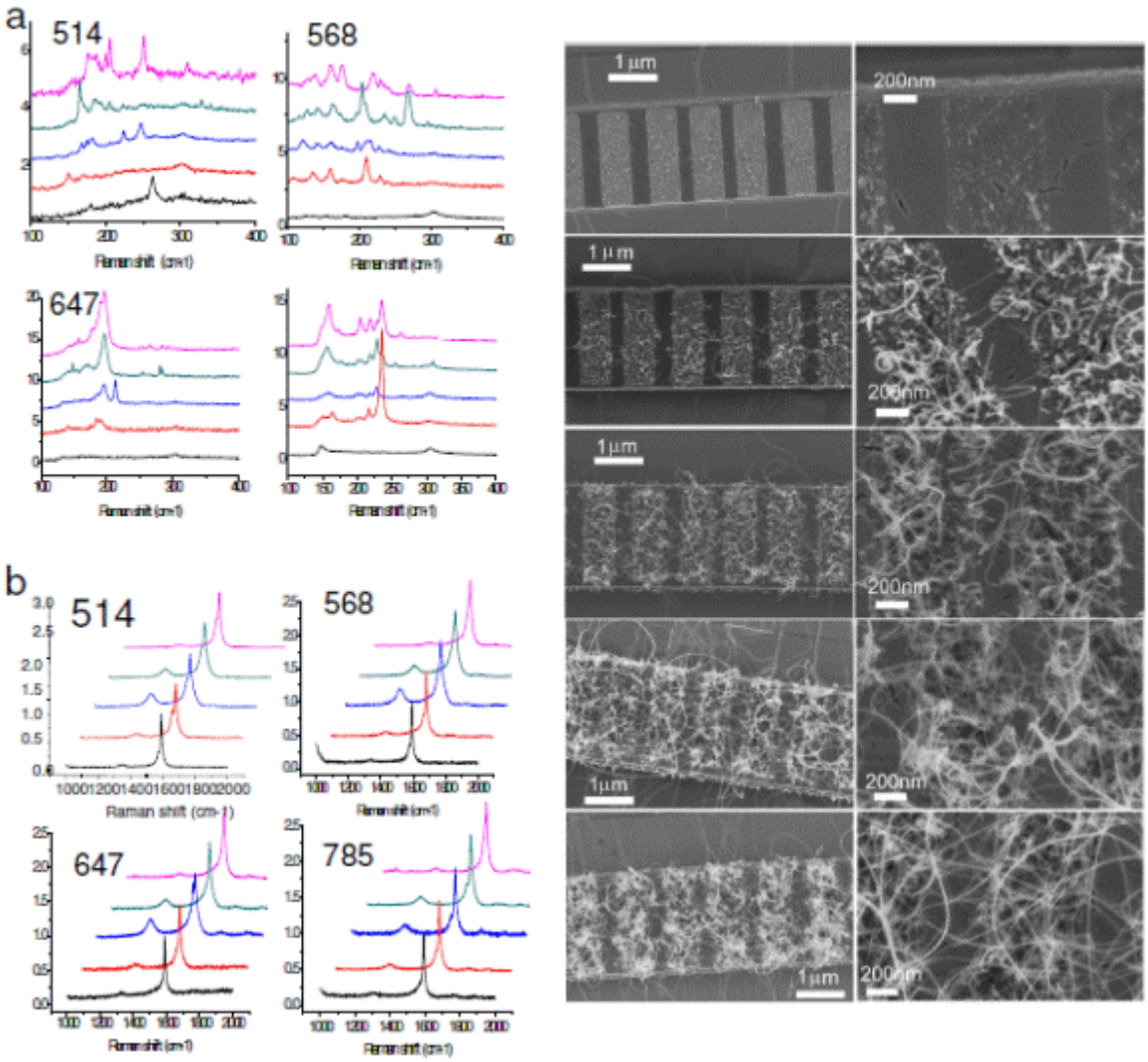

Figure 4. (a), (b) Raman spectra obtained from in situ measurement in the growth chamber for four different wavelengths (growth temperature 800 ^{o}C). The growth time increases in each plot from bottom to top. Spectra were measured for 5 s, 15 s, 1 min, 5 min and 10 min growth. (a) RBM region, (b) G–D mode region (spectra normalised to same G-peak height). (c) SEM pictures of the substrate corresponding to growth times as studied in the Raman experiments. From top to bottom the pictures illustrate growth after 5 s, 15 s, 1 min, 5 min and 10 min.

The higher wavenumber range of the Raman spectra showing the G – and D-peaks is shown in Figure 4(b) where the spectra have been normalised to the same G-peak height. The spectra do not change very much with increasing growth time. The main G+ and G- peaks remain at the same positions just increasing slightly in width as the density of nanotubes on the substrate increases. The most striking feature is the appearance and then disappearance of the D-peak. The relative intensity of the D-peak reaches a maximum for a growth time

of 1 minute. The fitted G/D ratio is plotted in Figure 5(a) as a function of growth time for the four different laser wavelengths. The trend is very clear and is reproduced for each laser wavelength. This may be indicating the formation of an amorphous carbon layer at the substrate or may be indicating a stage of rapid nucleation and growth yielding structures with a relatively large number of defects. Interestingly, as the nanotubes continue to grow, the D-peak decreases again in intensity, suggesting that the nanotubes are undergoing a self-annealing process as the growth continues. This is clearly seen in Figure 5(b) where the absolute intensities, using 647 nm laser excitation, are plotted for 5 minutes and 10 minutes growth. There is no evidence from the Raman spectra for the development of multi-walled nanotubes (although this cannot be totally ruled out at present) or significant carbon deposits for longer growth times.

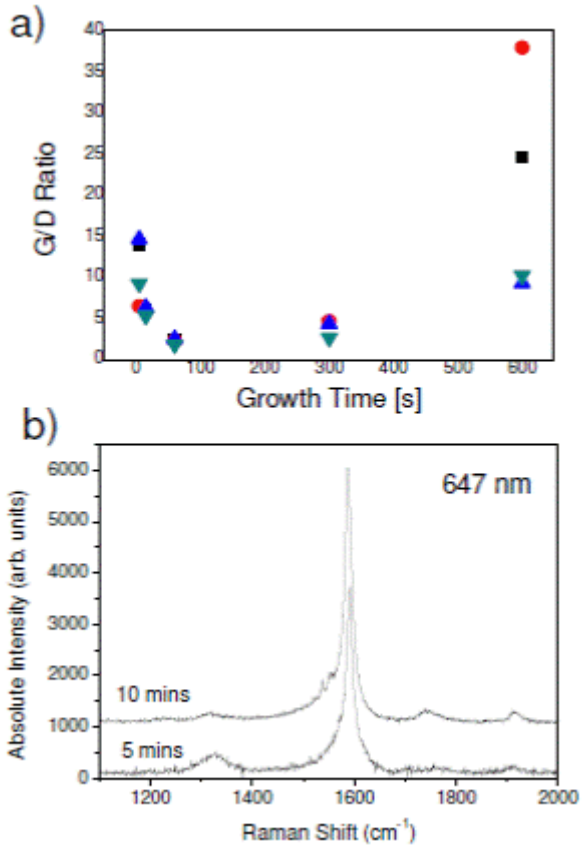

Figure 5. (a) Plot of the G/D ratio determined by fitting the spectra in (b) as a function of growth time. The different symbols represent measurements at different laser wavelengths (squares: 514 nm, circles: 568 nm, up-triangles: 647 nm, down-triangles: 785 nm). (b) Absolute intensity in the G–D region for 5 min and 10 min growth, using a laser excitation wavelength of 647 nm. The absolute intensity of the D-peak decreases as the growth time increases from 5 to 10 min.

References

[1] Y. Makita, S. Suzuki, H. Kataura, Y. Achiba, Eur. Phys. J D **34** (2005) 287.

[2] A.A. Puretzky, D.B. Geohegan, S. Jesse, I.N. Ivanov, G. Eres, Appl. Phys. A **81** (2005) 223.

[3] S. Chiashi, Y. Murakami, Y. Miyauchi, S. Maruyama, Chem. Phys. Lett. **386** (2004) 89.

[4] K. Kaminska, J. Lefebvre, D.G. Austing, P. Finnie, Nanotechnol. **18** (2007) 165707.

[5] T. de los Arcos, F. Vonau, M.G. Garnier, V. Thommen, H.G. Boyen, P. Oelhafen, M. Duggelin, D. Mathis, R. Guggenheim, Appl. Phys. Lett. **80** (2002) 2383.

[6] E.O Sunden, T.L. Wright, J. Lee, W.P. King, S. Graham, Appl. Phys. Lett. **88** (2006) 033107.

[7] M.S. Bell, K.B.K. Teo, R.G. Lacerda, W.I. Milne, D.B. Hash, M. Meyyappan, Pure Appl. Chem. **78** (2006) 1117.

[8] M. Jönsson, O.A. Nerushev, E.E.B. Campbell, Appl. Phys. A **88** (2007) 261.

[9] S. Dittmer, O.A. Nerushev, E.E.B.Campbell, Appl. Phys. A **84** (2006) 243.

[10] O. Englander, D. Christensen, L. Lin, Appl. Phys. Lett. **82** (2003) 4797.

[11] C. Hierold, A. Jungen, C. Stampfer, T. Helbling, Sensors and Actuators A: Physical **136** (2007) 51.

[12] S. Dittmer, S. Mudgal, O. A. Nerushev, E.E.B. Campbell, submitted to Low Temp. Phys.

[13] J. Bond, J. Lefebvre, D.G. Austing, L. Tay, P. Finnie, Nanotechnol. **18** (2007) 135603.

[14] D.G. Austing, J. Lefebvre, J. Bond, P. Finnie, Appl. Phys. Lett. **90** (2007) 103112.